Histological and micro Computed Tomography analysis of a femoral stress fracture associated with prolonged bisphosphonate use

Matthijs Paul Somford[1]
Leo J van Ruijven[2]
Peter Kloen[3]
Astrid D Bakker[2]

[1] Department of Orthopaedic Surgery, Martini Hospital, Groningen, The Netherlands
[2] Department of Oral Cell Biology and Functional Anatomy, ACTA-University of Amsterdam and VU University Amsterdam, MOVE Research Institute Amsterdam, Amsterdam, The Netherlands
[3] Department of Orthopaedic Surgery, AMC, Groningen, The Netherlands

Address for correspondence:
Matthijs Paul Somford
Department of Orthopaedic Surgery
Martini Hospital
Van Swietenplein 1
9728NT Groningen, The Netherlands
Tel: +31624881380
E-mail: mp_somford@hotmail.com

Summary

***Background*. The origin of atypical femoral fractures (AFF) associated with bisphosphonate therapy remains to be elucidated. In this study, a biopsy of an AFF site is analyzed to determine whether microdamage and/or morphological changes are present in the area of the AFF.**
***Material and methods*. Cortical bone from an AFF region was obtained during a preventive stabilization in a patient with a symptomatic AFF. This bone was scanned using microCT (resolution=0.01 mm), stained with basic fuchsin and analyzed histologically.**
***Results*. The diameter of the Haversian canals was higher in the vicinity of the AFF compared to the bone further away from the AFF. The bone mineral density within the cortex ranged from 1020 to 1080 mg HA/cm^3. We observed penetration of basic fuchsin into the matrix, which is a tell-tale sign of diffuse damage.**
***Discussion*. The higher diameter of haversian canals is likely to result in higher local stresses and consequently increased microdamage. The diffuse microdamage in the biopsy may furthermore be directly related to bisphosphonate use, preventing repair of microdamage, and consequently the development of the AFF.**
***Conclusion*. Increased porosity of the cortex and accumulation of microdamage might have lead to a stress fracture and ultimately a complete AFF.**

KEY WORDS: bisphosphonate; spontaneous fracture; histology; atypical femoral fracture.

Introduction

A possible long-term effect of bisphosphonate use is a stress fracture of the proximal femur progressing into a complete atypical femoral fracture (AFF) (1-7). The mechanism involved in the development of these atypical femur fractures remains unclear, and the bone pathology at the fracture site has not yet well been established (8). The aim of this study was to carefully characterize the region surrounding the stress fracture of a patient with respect to the volumetric Bone Mineral Density (vBMD), the diameter of the Haversian channels, and the number of microcracks.

Case

A 62-year-old patient was seen in our outpatient clinic in 2012 with left mid-thigh pain since 4 weeks without preceding trauma. Medical history included myasthenia gravis since 2004 treated with prednisolone 12.5 mg/day and osteopenia diagnosed with DXA-scans in 2008 and treated with alendronate 70 mg/week and calcium carbonate 500 mg and vitamin D 800iE on a daily basis. This treatment had been given for four years at the moment of presentation. X-ray examination revealed a lateral subtrochanteric stress fracture (supplementary material 1A).
A preoperative DXA scan of the left proximal femur and lumbar vertebra L1 revealed normal bone density. The patient was treated with an intramedullary osteosynthesis combined with the excision of the stress fracture area. Bisphosphonate treatment was discontinued and parathyroid hormone 100 mcg daily was started.
At three years follow up she had no complaints of her leg and the fracture gap was filled completely (supplementary material 1B).

Materials and methods

Informed consent was obtained from the patient before processing the bone biopsy (surgical waste material). The biopsy was fixed in 4% formaldehyde, and dehydrated for 7 days in 70% alcohol. Subsequently, microCT was performed on the biopsy, before being further processed for histological analysis.

Ethical approval

Ethical committee approval is not applicable since the study considers surgical waste material. Patient consent was retrieved.

MicroCT

For micro computed tomography (microCT) analysis the biopsy was placed in a cylindrical specimen holder (19.9 mm diameter) and scanned with the μCT 40 (Scanco Medical

AG, Brüttisellen, Switzerland). The integration time was set at 1000 ms, the beam intensity at 55 kV, the current at 145 mA, and the resolution at 0.010 mm. Three-dimensional reconstructions were made with the cone-beam reconstruction algorithm. The contours of the fragment of bone were manually traced, excluding the main fracture and tiny cracks surrounding it as well as the fracture callus. Subsequently, 30 subvolumes were defined in the scan using a rectangular grid. Each subvolume was segmented using the standard procedure (sigma=0.5, support=1, threshold=613 mg HA/cm^3) and both the vBMD and the mean diameter of the Haversian channels were calculated using the standard evaluation software (UCT_Evaluation v6.5-3, Scanco Medical A.G., Brüttisellen, Switzerland). Finally, the contours of the fracture callus present on the endocortical and periosteal surfaces of the cortical bone were manually traced and the vBMD of these newly formed bone layers were compared to that of the cortical bone matrix.

Histology

For histology, the biopsy was incubated en block in a series of 1% basic fuchsin (Sigma-Aldrich, St. Louis, MO, USA) solutions in alcohol (supplementary material 2), after which the biopsy was rinsed in 100% alcohol for 1h. Subsequently, the dehydrated and undecalcified biopsy was embedded in methylmethacrylate (MMA). Sections of 5µ3m thickness were made every 500 μm over a total distance of approximately 4 cm. Sections were analyzed using light microscopy for the presence of microdamage.

Results

MicroCT

The stress fracture was clearly visible on the microCT scans (Figure 1B). Trabecular bone-like material, likely representing the persisting fracture callus, was clearly visible on the endosteal and periosteal surface of the biopsy (Figure 1A, B). This trabecular material contained woven bone (data not shown), and was calcified, but much less so than the native bone matrix, i.e. the mineral density distribution of the old bone was on average 1070 mg HA/cm^3, *versus* 787 mg HA/cm^3 for the bone formed on the endosteal and periostal surface.

The vBMD slightly varied in the endosteal-periosteal direction (x-axis in Figure 3) as well as in the proximal-distal direction within the cortical bone (Vol0 to vol4 in Figure 3), but this variation did not exceed the margin of error for the scan. The vBMD ranged from 1020 to 1080 mg HA/cm^3 (Figure 3a).

Haversian channels on the periosteal side of the biopsy were of a normal size (0.050 - 0.080 mm; right hand of the x-axis in Figure 3B) (9, 10). On the endosteal side (Figure 3; left hand of the x-axis in 3b), especially in the neighbourhood of the crack (Figure 3; vol0 to vol2 in 3b), the average diameter was markedly higher than on the periosteal side (Figure 3b; 0.260-0.330 mm).

Histology

The stress fracture was clearly visible in the histological sections (Figure 4). In the region around the fracture, linear microcracks were visible and basic fuchsin (red) had penetrated the matrix around the fracture. On the periosteal and endosteal side of the cortex a layer of bone was visible with a trabecular appearance, similar to the virtual 2 dimensional microCt images (Figure 2). Osteoclasts were not detectable due to the intense staining with basic fuchsin. There was a lot of erythrocytes visible in the specimen. No blood vessels were observed within the fracture.

Discussion

An interesting observation was the large osteonal diameter at the endosteal side of the bone (11). The increased osteon diameter near the fracture site is unlikely to be an effect of the fracture, because the bisphosphonates will have stopped the osteoclast activity even before the fracture occurred. Bisphosphonates stop the resorption of bone by osteoclasts but might thereby also be influencing the osteoblasts through disturbed osteoclast-osteoblast coupling (12).

The vBMD within the cortex ranged from 1020 to 1080 mg HA/cm^3 and seemed to be slightly lower on the periosteal surface. However, these differences in vBMD are so small, that it cannot be reliably concluded that mineralization is lower on the periosteal surface than the endosteal surface.

Arrest of natural remodelling in the bone can lead to an accumulation of unrepaired microdamage in the matrix, leading to fatigue fractures (13, 14). We observed penetration of basic fuchsin into the matrix, which is a tell-tale sign of diffuse damage. It is possible that this microdamage pre-existed prior to the occurrence of the fracture, and has led to the development of the stress fracture (personal communication with Prof. M.B. Schaffler), but it is impossible to exclude the possibility that the microdamage is the effect rather than the cause of the stress fracture. It should be noted that, at the site where the bone was removed, marks of the point of the clamp with which the bone was removed are visible in the histological sections without microcracks, suggesting that damaging the bone does not automatically lead to microdamage in the matrix, and this strengthens the suggestion that the damage preceded the fracture.

The fracture callus was clearly present at 4 weeks after the initial presentation, although the fracture must have been present for a longer period of time. During normal fracture healing, the peak of soft callus is found at 7-9 days and calcified callus appears from 2-6 weeks after fracture and can persist for weeks until bony union (15). The callus in our biopsy had a trabecular-like appearance, and showed no signs of being removed (absence of scalloped surfaces) or remodelled. A limitation of our study is that we do not have the exact date that the stress fracture arose. Unfortunately another limit is that because of our staining method osteoclasts were not visible, but Vigorita et al. suggest they may be present, albeit not active (17). It is not possible to determine precisely whether the callus consisted of bone or calcified cartilage by the methods used in the current study. On microCT the calcification of the callus was lower than that of mature bone. On histology the callus contained woven bone rather than lamellar bone, as would have been expected in mature bone matrix. The findings suggest that the first stages of healing (inflammation, attraction of stem cells) had occurred, but had stopped there. The use of bisphosphonates has possibly prevented progression of the healing by blocking the osteoclast. Blocking of osteoclasts prevents the resorption of damaged bone, but may also impair new bone formation, since resorption of the matrix by osteoclasts releases growth factors such as insulin-like growth factor 1 and

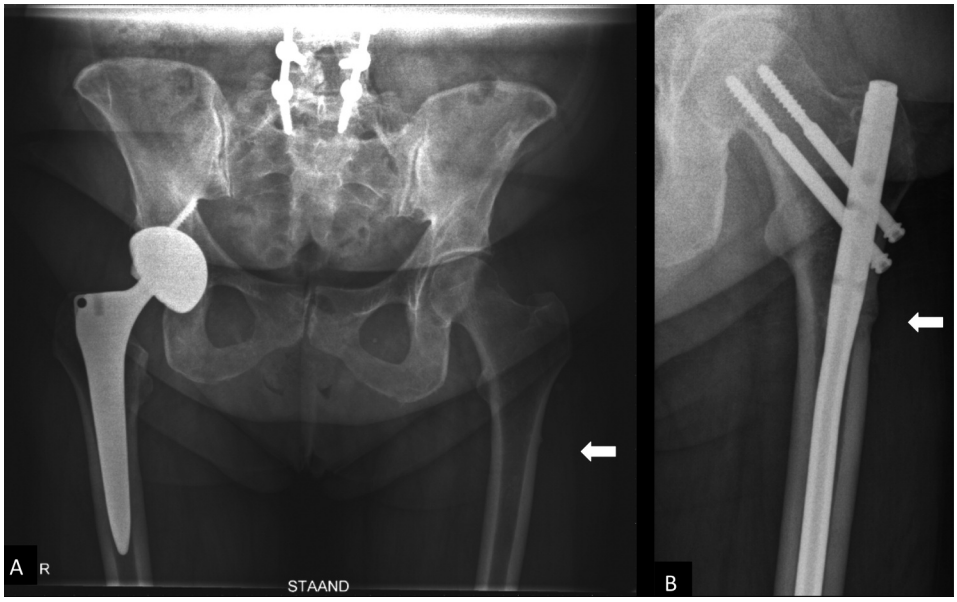

Figure 1 - A) AP pelvis X-ray with cortical thickening (arrow) on the lateral side of the left femur. B) AP pelvis at 1 year after treatment of the AFF with intramedullary fixation in place.

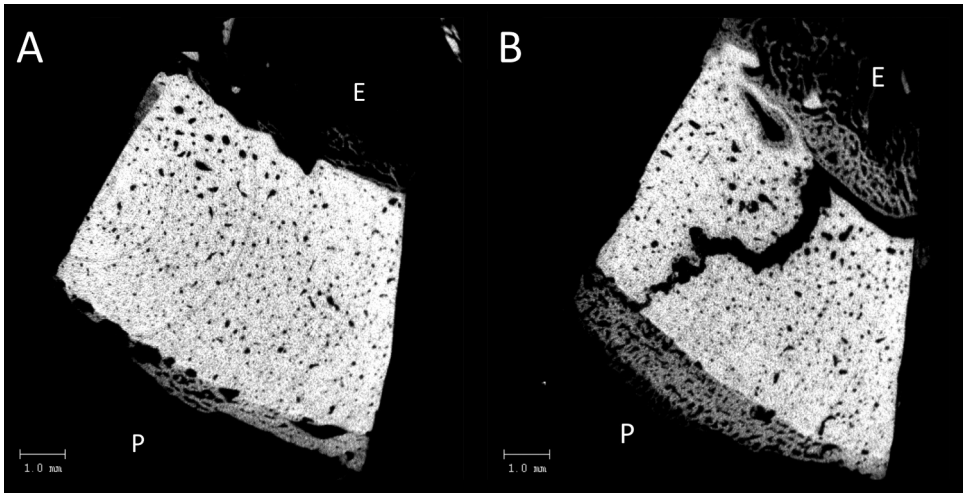

Figure 2 - A) Virtual 2 dimensional section through the 3 dimensional microCT scan of the entire biopsy. The endosteal side is marked with 'E'. Note the apparently wider Haversian canals on the endosteal side. The fracture is not visible in this virtual section. B) Virtual 2 dimensional section through the 3 dimensional microCT scan of the entire biopsy. The endosteal side is marked with 'E' and periosteal side with 'P'. The fracture is clearly visible in this virtual section.

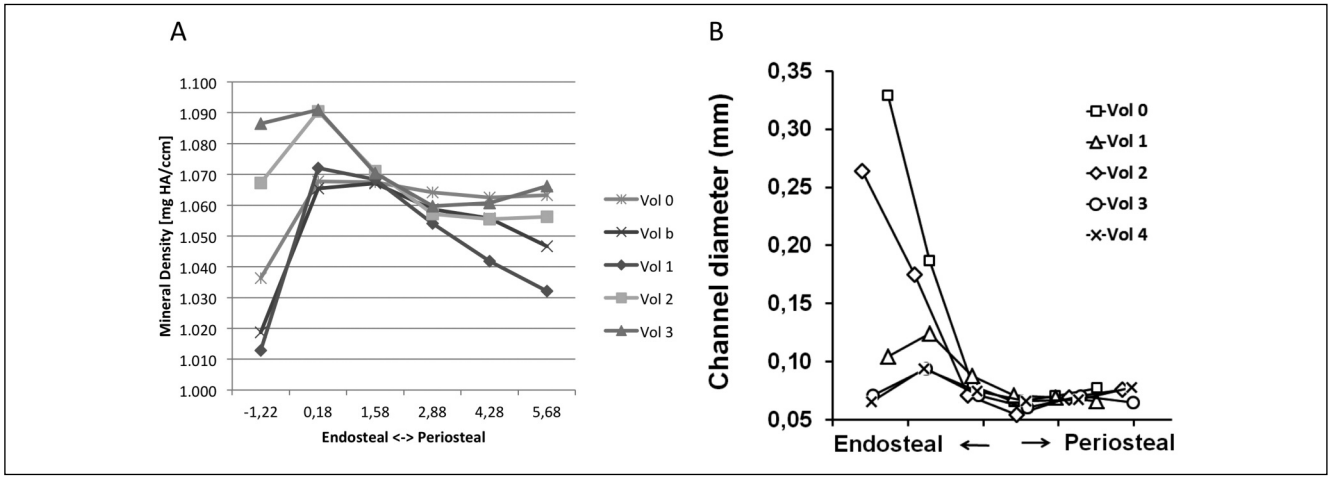

Figure 3 - A) Quantification of volumetric Bone Mineral Density in the 30 subregions defined within the biopsy. B) Quantification of Haversian canal diameter in the 30 subregions of the biopsy. The fracture runs through vol0, vol1 and vol2, while vol3 and vol4 are situated further away from the fracture. Points on the left hand side of the graph are situated in their respective volumes near the endosteal surface of the biopsy, while points on the right hand of the graph are situated near the periosteal side of the biopsy.

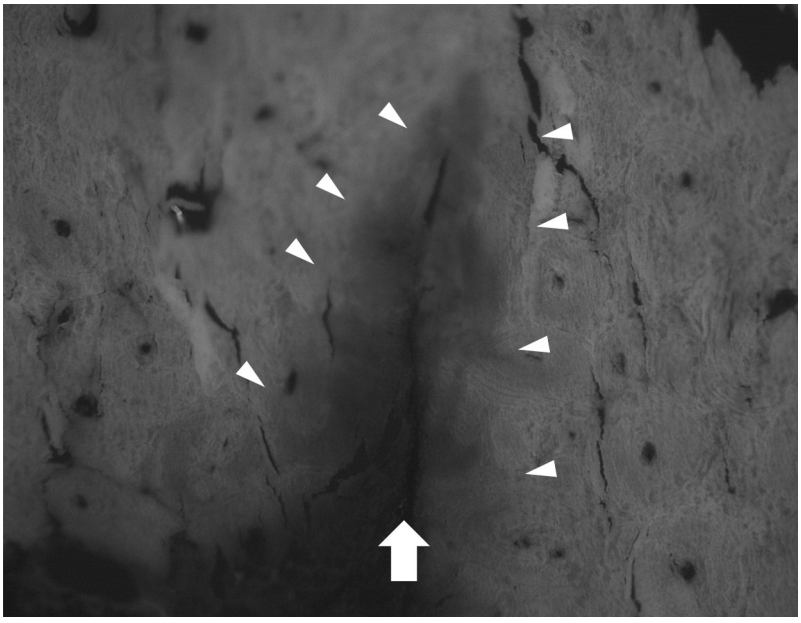

Figure 4 - Histological section of the specimen with clearly visible fracture (arrow). Fuchsin (red) penetration in the matrix is clearly visible (arrowheads) indicating the presence of microdamage. Microcracks (red) following cement lines of osteons are visible on the left hand side of the picture.

bone morphogenetic proteins among other factors that stimulate osteoblast activity (12).

There was a lot of erythrocytes visible, which most likely were washed into the fracture when the biopsy was taken, as no blood vessels were observed within the fracture. This again suggests that the fracture it self was not progressing beyond a certain stage of the healing process. It has been described that fracture healing is delayed in people after prolonged bisphosphonate use and specifically after AFF (18-20).

Acknowledgments

We thank the expert help of Marion van Duin for preparing the histological sections and performing the histological analysis.

Conflict of interest

Matthijs Paul Somford, Leo J van Ruijven, Peter Kloen, and Astrid D Bakker declare that they have no conflict of interest.

References

1. Favus MJ. Bisphosphonates for osteoporosis. N Engl J Med. 2010; 363:2027-2035. doi: 10.1056/NEJMct1004903.
2. Somford MP, Thomassen BJW, Draijer WF. Femur fractures caused by long-term bisphosphonate therapy. Ned Tijdschr Geneeskd. 2010; 154:A1218.
3. Somford MP, Draijer FW, Thomassen BJW, et al. Bilateral fractures of the femur diaphysis in a patient with rheumatoid arthritis on long-term treatment with alendronate: clues to the mechanism of increased bone fragility. J bone Miner Res Off J Am Soc Bone Miner Res. 2009;24:1736-1740.
4. Shane E, Burr D, Ebeling PR, et al. Atypical subtrochanteric and diaphyseal femoral fractures: report of a task force of the American Society for Bone and Mineral Research. J Bone Miner Res. 2010;25:2267-94. doi: 10.1002/jbmr.253.
5. Saleh A, Hegde V V, Potty AG, Lane JM. Bisphosphonate therapy and atypical fractures. Orthop Clin North Am. 2013;44:137-151. doi: 10.1016/j.ocl.2013.01.001.
6. Jo YR, Kim HW, Moon SH, Ko YJ. A case report of long-term bisphosphonate therapy and atypical stress fracture of bilateral femur. Ann Rehabil Med. 2013;37:430-432. doi: 10.5535/arm.2013.37.3.430.
7. Bissonnette L, April P-M, Dumais R, et al. Atypical fracture of the tibial diaphysis associated with bisphosphonate therapy: A case report. Bone. 2013;56:406-9. doi: 10.1016/j.bone.2013.07.012.
8. van Ruijven LJ, Mulder L, van Eijden TMGJ. Variations in mineralization affect the stress and strain distributions in cortical and trabecular bone. J Biomech. 2007;40:1211-1218. doi: 10.1016/j.jbiomech.2006.06.004.
9. Johnson L. Morphologic analysis of pathology. In: Frost H (ed) Bone Biodyn. Little, Brown and Company, Boston, MA, 1964, pp 543-654.
10. Agerbaek MO, Eriksen EF, Kragstrup J, et al. A reconstruction of the remodelling cycle in normal human cortical iliac bone. Bone Miner. 1991;12:1011-12.
11. Frost HM. Skeletal structural adaptations to mechanical usage (SATMU): 2. Redefining Wolff's law: the remodeling problem. Anat Rec. 1990;226:414-422. doi: 10.1002/ar.1092260403.
12. Pederson L, Ruan M, Westendorf JJ, et al. Regulation of bone formation by osteoclasts involves Wnt/BMP signaling and the chemokine sphingosine-1-phosphate. Proc Natl Acad Sci. 2008;105:20764-20769. doi: 10.1073/pnas.0805133106.
13. Yamagami Y, Mashiba T, Iwata K, et al. Effects of minodronic acid and alendronate on bone remodeling, microdamage accumulation, degree of mineralization and bone mechanical properties in ovariectomized cynomolgus monkeys. Bone. 2013;54:1-7. doi: 10.1016/j.bone.2013.01.016.
14. Schaffler MB. Role of bone turnover in microdamage. Osteoporos Int. 2003;14 Suppl 5:S73-7; discussion S77-80. doi: 10.1007/s00198-003-1477-1.
15. Hoerth RM, Seidt BM, Shah M, et al. Mechanical and structural properties of bone in non-critical and critical healing in rat. Acta Biomater. 2014;10:4009-4019. doi: 10.1016/j.actbio.2014.06.003.
16. Marsell R, Einhorn TA. The biology of fracture healing. Injury. 2011;42:551-555. doi: 10.1016/j.injury.2011.03.031.
17. Vigorita VJV, Silver JS, Eisemon EOE. Osteoclast abnormalities in fractured bone during bisphosphonate treatment for osteoporosis: a case report. Skeletal Radiol. 2012;41:861-865. doi: 10.1007/s00256-012-1407-4.

18. Kang JS, Won YY, Kim JO, et al. Atypical femoral fractures after anti-osteoporotic medication: a Korean multicenter study. Int Orthop. 2014;38:1247-1253. doi: 10.1007/s00264-013-2259-9.
19. Molvik H, Khan W. Bisphosphonates and their influence on fracture healing: a systematic review. Osteoporos Int. 2015;26:1251-1260. doi: 10.1007/s00198-014-3007-8.
20. Egol KA, Park JH, Rosenberg ZS, et al. Healing delayed but generally reliable after bisphosphonate-associated complete femur fractures treated with IM nails. Clin Orthop Relat Res. 2014;472:2728-2734. doi: 10.1007/s11999-013-2963-1.